J Mol Model (2012) 18:4333–4341
DOI 10.1007/s00894-012-1436-x

ORIGINAL PAPER

Molecular interactions of c-ABL mutants in complex with imatinib/nilotinib: a computational study using linear interaction energy (LIE) calculations

Elen Gomes Pereira · Miguel Ângelo Martins Moreira · Ernesto Raúl Caffarena

Received: 4 November 2011 / Accepted: 17 April 2012 / Published online: 9 May 2012

Abstract In spite of the effectiveness of Imatinib for chronic myeloid leukemia (CML) treatment, resistance has repeatedly been reported and is associated with point mutations in the *BCR-ABL* chimeric gene. To overcome this resistance, several inhibitors of BCR-ABL tyrosine kinase activity were developed. In this context, computational simulations have become a powerful tool for understanding drug-protein interactions. Herein, we report a comparative molecular dynamics analysis of the interaction between two tyrosine kinase inhibitors (imatinib or nilotinib) against wild type c-ABL protein and 12 mutants, using the semi-empirical linear interaction energy (LIE) method, to assess the feasibility of this approach for studying resistance against the inhibitory activity of these drugs. In addition, to understand the structural changes that are associated with resistance, we describe the behavior of water molecules that interact simultaneously with specific residues (Glu286, Lys271 and Asp381) of c-ABL (wild type or mutant) and their relationship with drug resistance. Experimental IC50 values for the interaction between imatinib, wild type c-ABL, and 12 mutants were used to obtain the proper LIE coefficients (α, β and γ) to estimate the free energy of the binding of imatinib with wild-type and mutant proteins, and values were extrapolated for the analysis of the nilotinib/c-ABL interaction. Our results indicate that LIE was suitable to predict the superior inhibitory activity of nilotinib and the resistance to inhibition that was observed in c-ABL mutants. Additionally, for c-ABL mutants, the observed number of water molecules being turned over while interacting with amino acids Glu286, Lys271 and Asp381 was associated with resistance to imatinib, resulting in a less effective inhibition of the kinase activity.

Keywords BCR-ABL · Chronic myeloid leukemia · Drug resistance · Imatinib · Linear interaction energy · Nilotinib

E. G. Pereira
Laboratório Nacional de Computação Científica, LNCC,
Av. Getúlio Vargas, 333,
Petrópolis, RJ, Brazil 25651-075

M. Â. M. Moreira
Genetics Division, Instituto Nacional de Câncer, INCA,
André Cavalcanti 37,
Rio de Janeiro, RJ, Brazil 20231-050

E. R. Caffarena (✉)
Programa de Computação Científica, Fundação Oswaldo Cruz,
Av. Brasil 4365. Manguinhos,
Rio de Janeiro, RJ, Brazil 21040-360
e-mail: ernesto@fiocruz.br

Introduction

Detected in 1960, the Philadelphia (Ph) chromosome was the first chromosome anomaly found to be associated with a malignancy: chronic myeloid leukemia (CML). In 1973, the Ph chromosome was found to be the result of a reciprocal translocation between the long arms of chromosome 9 and 22, a consequence of which was that a chimeric gene *BCR-ABL* was formed from the fusion of the *BCR* gene, at 22q11, and the proto-oncogene *c-ABL* (coding for a Tyrosine kinase), at 9q34.1. The Ph chromosome is found in 95 % of the CML cases while the chimeric BCR-ABL protein, with an uncontrolled kinase activity, is the cause of CML [1]. During the late 1990's, a series of synthetic molecules were developed and tested for specifically inhibiting the BCR-ABL kinase activity, and imatinib (STI-571 or Gleevec) was the first of these drugs that was approved and used as a therapeutic agent for CML [2–4]. However, despite its effectiveness in CML treatment, primary or secondary resistance was reported in several patients. The mechanisms

triggering resistance are probably heterogeneous, and two such mechanisms have been described in in vivo studies: amplification of the *BCR-ABL* gene and amino acid substitutions [5] resulting from recurrent point mutations [6–8] at the c-ABL catalytic site, at the activation loop (A-loop) and at the ATP phosphate-binding loop (P-loop).

Crystallographic analyses showed that imatinib binds to the ABL kinase domain in a catalytically inactive conformation, often referred as the 'DFG' out conformation (D=Asp381, F=Phe382, and G=Gly383). This motif flips out to make a channel beyond the gatekeeper residue (Thr315) for the benzamide and N-methylpiperazine groups of imatinib [9, 10]. The P-loop folds down to form a cage around the pyridine and pyrimidine groups of imatinib, maintaining extensive hydrophobic interactions around the inhibitor [11]. The occurrence of point mutations at the DFG motif or at the P-loop increases the free energy of the imatinib-ABL complex [12]. Hence, a detailed analysis of point mutations that modify the stability of the inactive conformation could provide invaluable information about the relevance of these interactions.

To overcome the resistance to imatinib, a new series of Tyrosine kinase inhibitors was developed, including the following: nilotinib (AMN107) [13, 14], dasatinib (BMS-354825) [15–19], bosutinib (SKI-606) [15], INNO-406 (NS-187), AZD0530, MK-0457 (VX-680) [20], and PHA-739358. The development of nilotinib (AMN107; Novartis), a phenylaminopyrimidine derivative, resulted in an inhibitory molecule that was 30-fold more potent. Nilotinib showed an inhibitory capacity against 32 out of the 33 forms of BCR-ABL mutants that were resistant to imatinib and was approved for CML treatment [21, 22].

Today, methods based on molecular-mechanics, such as comparative modeling and molecular dynamics, are reliable approaches to simulate the effects of specific mutations on the affinity between ligands and receptors. Additionally, computational simulations can be used to understand biological systems because they are a rapid and powerful way to investigate interactions at the atomic level. Among these simulations, Pricl et al. [23] showed that a series of protein/drug interactions that are beyond those affecting specifically the amino acid substitution site (*e.g.*,:T315I) account for a loss of imatinib stability at the c-ABL kinase binding site. More recently, Aleksandrov and Simonson [24] have studied the c-ABL protein structure, analyzing the dynamics and thermodynamics of the interaction with imatinib and four similar analogues. Calculations were performed for different protonation states of imatinib, demonstrating that the protonated inhibitor effectively binds to c-ABL. Furthermore, the same authors [25] used the linear interaction energy (LIE) [26] with the Poisson-Boltzann free energy method (PBSA) to elucidate protein-imatinib interactions when the kinase domain is in the DFG-out conformation, evaluating its ability to select or induce this conformation.

Molecular dynamics (MD) allows for evaluation of the relevance of specific solvent molecules involved in the maintenance protein structure as well as for the interaction between protein and ligand [27–31]. Additionally, MD analysis of mutations affecting protein function was associated with disruption of water networks [32]. In the case of c-ABL, Schindler et al. [3] suggested that specific water molecules could help stabilize its binding with the imatinib kinase inhibitor. These authors call attention to a water molecule that interacts with the residues Glu286, Lys271, and Asp381 when c-ABL is in the inactive form. The aspartic acid residue is part of the above mentioned DFG motif, being conserved in different kinase domains, and coordinates a magnesium ion associated with the ATP molecule [33]. Taken together, these findings suggest that this specific water molecule (or water molecules), occupying this position, is crucial for maintaining a stable interaction between c-ABL and its inhibitor.

Here, we report on a comparative analysis of the free energy of binding of imatinib and nilotinib with the c-ABL protein, using the semi-empirical LIE method [26] for assessing the feasibility of this approach to study the resistance of the c-ABL mutants against the inhibitory activity of these drugs. This methodology is considered useful because of its simplicity, its reduction of the system size, its representation of solvents through explicit water models, the possibility of calculating absolute binding energies and its use of short simulation times [34, 35]. We conducted analyses with the c-ABL protein structure and 12 mutants (based on wild type protein structures) that were previously associated with clinical and/or in vitro resistance. The methodology was calibrated to account for the behavior of the mutants in a complex with imatinib and then was extrapolated to nilotinib in a complex with the same mutants, considering the high degree of similarity between both ligands. In addition, to evaluate the relevance of the water molecules for the interaction between c-ABL and the two inhibitors, we described the behavior of the water molecules, which simultaneously interact with the Glu286, Lys271, and Asp381 residues in the wild type and selected mutants of c-ABL.

Computational details

The complex of the ABL kinase domain and imatinib, obtained by X-ray crystallography with a resolution of 1.75 Å, was used as the initial structure for the simulations (PDB code 1OPJ) [36]. The initial coordinates for the nilotinib-ABL kinase domain complex were obtained from a homology model, using the 1OPJ file as a template and using the SPDB-VIEWER program [37]. It is worth mentioning that, despite the fact that the 3CS9 [38] PDB entry is in a complex with nilotinib, four important residues between β3

and the catalytic region (Glu275, Asp276, Thr277 and Met278) are not elucidated in the crystal. The full identity between both sequences that are associated with the high resolution of the template, namely 1OPJ and 3CS9, permitted the construction of the structural model for the kinase domain in complex with nilotinib, by simply adding and optimizing the missing residues. The geometries were optimized with 1000 steps of a steepest descent algorithm. Figure 1 shows the initial conformations of WT c-ABL binding site in complex with imatinib and nilotinib, respectively.

The 12 mutations (M244V, M244I, L248R, Q252H, Y253H, E255K, T315I, T315S, M351T, M351I, L384M and G398R; identification of amino acids residues are respective to the c-ABL 1a protein) of the c-ABL kinase domain were incorporated into the initial wild type structures (WT) by using the SPDB-VIEWER program [37]. Absolute free energy estimates were computed using the LIE method with the software package Q [39] and the Gromos96 (version G43a1) united atom force field [40], and the estimates account for only the polar and aromatic hydrogens. The water molecule involved in the network of hydrogen bonds encompassing residues Lys271, Glu286, Asp381 and the acid amide group of imatinib (see Schindler et al. [3]) was maintained.

The topologies of the ligands were generated by the PRODRG server [41] and were adapted to the Q program. Atomic partial charges corresponded to the MMFF94 force field [42].

The systems, receptors with imatinib or nilotinib, were hydrated with the SPC [43] water model within a 20 Å radius sphere, which was centered at the center of mass of the ligand. Non-bonded interactions across the boundary were excluded and inner electrostatic and Lennard-Jones interaction energies were calculated without cut-off restrictions while long-range electrostatics were treated using a multipolar expansion [44]. Atoms outside the inner simulation sphere of 18.5 Å of radius were harmonically restrained to their initial positions with a 200 kcal mol^{-1} $Å^{-2}$ force constant.

The systems were heated from 1 to 300K using a stepwise scheme followed by an equilibration period to stabilize ligand-surrounding interactions before achieving the data collection phase. During the heating phase, heavy atoms of imatinib, nilotinib and the crystallographic water C_w (see below) were restrained to their initial positions using a harmonic potential with a force constant of 5 kcal mol^{-1} $Å^{-2}$. Application of a weak coupling external bath was necessary to set up the temperature at 300K, with a relaxation time of 10 fs [45].

The SHAKE [46] algorithm was used to constrain solute bonds and also angles of solvent molecules. The step size used in the equilibration and production phases of the simulations was 1 fs. Trajectories were collected over 5 ns and the free energy of binding was calculated (Eq. 1) over the last 3 ns. Analysis of the dynamical features of the solvent-protein interaction was performed based on the statistical inefficiency concept [47]. Atomic coordinates and velocities were saved every 0.25 ps.

The LIE methodology calculates the absolute binding free energy of a ligand as the change in free energy when the ligand is transferred from the solution (free state) to the solvated receptor binding site (bound state), which is composed of polar and non-polar contributions. The binding free energies were predicted in accordance with the following equation:

$$\Delta G_{bind} = \alpha(\langle U_{l-s}^{LJ}\rangle_{bound} - \langle U_{l-s}^{LJ}\rangle_{free}) + \beta(\langle U_{l-s}^{el}\rangle_{bound} - \langle U_{l-s}^{el}\rangle_{free}) + \gamma, \quad (1)$$

where U^{el} and U^{LJ} are the electrostatic and Lennard-Jones interaction energies, respectively, between a ligand and its surroundings in the binding site (bound state) and in aqueous solution (free state). The brackets <>'s denote MD ensemble averages over molecular dynamics simulation trajectories, and α, β and γ are empirical parameters.

Originally, for several receptor-ligand systems, Aqvist et al. [26] tested parameters that produced calculated binding free energies that were in good agreement with experimental data using a unique receptor that was bound to a set of different inhibitors. In subsequent studies of ligand binding, Hansson et

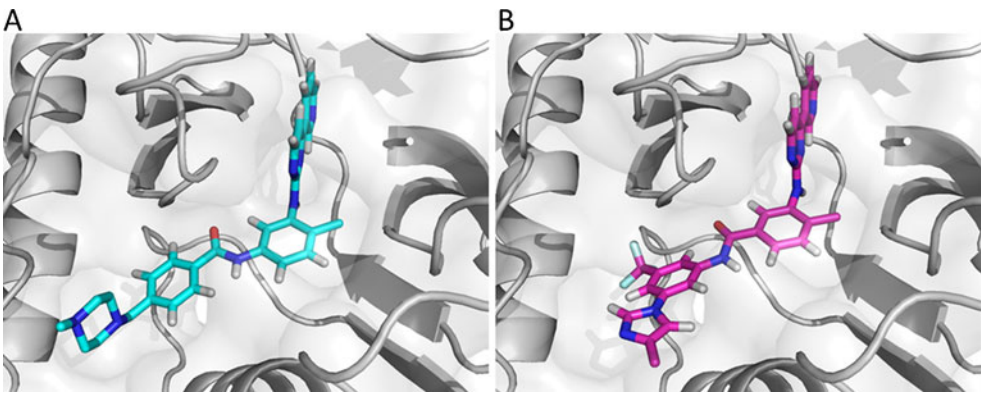

Fig. 1 Schematic drawing of interrelation between c-ABL protein and inhibitors imatinib (**a**) and nilotinib (**b**). The inhibitors are located tightly in the center of the active site of c-ABL

al. [48] determined a suitable set of β electrostatic parameters according to the physicochemical characteristics of the ligand together with the non-polar value of α=0.181, to adequately reproduce the free energies of binding for a variety of ligand-protein systems. In our specific case, we have two structurally similar ligands (imatinib or nilotinib) and 12 mutants of the same receptor; therefore, the standard parameterization no longer holds. Thus, to provide a good estimation of the free energy, a set of empirical coefficients α, β, and γ was chosen by minimizing the error for the binding free energies of imatinib and the wild type receptor and its mutant forms (Eq. 2), by applying the Broyden-Fletcher-Goldfarb-Shannon algorithm, based on a leave-one-out cross-validation.

$$E(\alpha,\beta,\gamma) = \sum_i \left(\frac{\Delta G_{bind} - \Delta G_{\exp}}{\Delta G_{\exp}} \right)^2, \quad (2)$$

where ΔG_{bind} is defined by Eq. 1 and ΔG_{exp} is from the experimental data derived from Azam et al. [49]

Simulations were conducted under physiological conditions (pH ~ 7.0) and considered His252 to be protonated at the δ position, as suggested by Lee et al. [50] in previous work. Structural and dynamical analysis of water molecules at the crystallographic position, required to make a network of hydrogen bonds with Glu286, Lys271 and Asp381 (named here the Cw pocket), was performed to characterize its relevance for the process of ligand-receptor interaction. For this purpose, the residence time (τ) of a water molecule at the Cw pocket was estimated from the positive hits that were counted when a water molecule was located simultaneously at distances less than 3.3 Å from the carbonyl oxygen of Asp381, the NZ of Lys271, and the CD of Glu286. The residence times τ were calculated according to the following equation:

$$\tau = \frac{\sum_i^N n_i \tau_i}{\sum_i^N n_i}, \quad (3)$$

where N is the total number of counts and n_i is the number of counts of time τ_i, which is simply calculated as the sum of consecutive snapshots times the time-step.

Results and discussion

The mutations M244V, M244I, L248R, Q252H, Y253H, E255K, T315I, T315S, M351T, M351I, L384M and G398R, herein analyzed, were selected in view of their localization in different c-ABL protein domains (M244I, M244V, L248R, Q252H, Y253H, E255K at the P-loop region, T315I, T315S between the SH2 and SH3 domains, M351T, M351I at the SH2 domain, and L384M and G398R at the activation loop). All of the mutations (except for L248R) were previously described in patients with clinical resistance, with the T315I having the highest incidence. Mutations M351T, M351I, and L384M were not previously analyzed by computational approaches, and mutations T315I and L248R are associated with a higher resistance to different kinase inhibitors. During the simulations of wild type c-ABL in complex with both inhibitors, the root mean square deviation value did not exceed 3 Å.

Absolute free energies of binding

The LIE method was previously applied to evaluate the interactions between proteinases and its inhibitors, i.e., oligopeptides that differ from each other by amino acid substitution at the same position [51]. These studies showed that the standard LIE coefficients, used for binding between small drug-like molecules and proteins, were not suitable for protein-protein interactions. A set of empirical parameters (α, β, and γ) had to be calculated for estimating the ΔG binding values from the MD simulations performed using the LIE method. When that approach was applied, Almlof et al. [51] placed the center of the simulation sphere at the residue position that was mutated to different amino acids. In the present work, a slightly different strategy was employed. We considered the center of the simulation sphere to be the center of mass of the ligand for simulations comprising all of the mutants, and the coefficients of the LIE equation were fitted to represent the average of the contributions of 13 structurally similar receptors (the wild type and the 12 mutants) in binding with imatinib.

Because this approach is mostly dependent on the number of analyzed mutations, it was not possible to separate our limited sample into a training set and a test set. Therefore, we opted to use the leave-one-out method for cross-validation, resulting in a set of coefficients that minimizes the error E (α,β,γ) (Eq. 2) resulting in R^2=0.4. The low value of R^2 is a consequence of a limitation of the method, which works with a set of only 13 mutations located in different places. Even though, under such working conditions, the method presented an adequate R^2 value. Taking out the M351I mutation from the mutant protein set, we obtained a minimum error, resulting in the values 0.221, 0.033 and −1.258 for α, β and γ, respectively; these values were used for the subsequent analyses. Elimination of two or more mutants also resulted in a worse calibration. On the other hand, we also observed that larger simulation times (by extending an extra nanosecond) do not improve the quality of the model and instead resulted in an equivalent calibration with larger error values (data not shown).

Because the LIE methodology has proven to be useful for ligands with similar chemical structures [26], the α, β and γ values obtained for imatinib were employed to calculate the ΔG values of the c-ABL protein (the wild type and mutants)

in a complex with nilotinib. Table 1 lists the experimental and calculated values for the absolute binding free energy between imatinib/nilotinib and the c-ABL proteins (wild type and 12 mutants).

It can be observed that the values of the absolute free energy of binding for the mutations were well reproduced for imatinib, resulting in absolute unsigned errors between experimental and calculated values lower than 1.0 kcal mol^{-1}. The highest unsigned differences were 0.97, 0.82 and 0.79 kcal mol^{-1} for WT, M351I, and T315I, respectively. The difference between the minimal and maximal experimental ΔG values is approximately 2.1 kcal mol^{-1} and for the predicted ΔG values is approximately 1.3 kcal mol^{-1}. A comparison between the calculated ΔG from the WT and mutants did not show resistance for T315S, M244I, Q252H, and G398R. Our results were in agreement with experimental data that indicate a weaker imatinib potency with respect to nilotinib for different mutations [27], except for T315S and E255K. The ΔΔU values between the bound and free states of the ligands are shown in Fig. 2.

The most important contribution to free energy was provided by the non-polar terms of the equation, which reflect the stability of the drugs inside the ligand binding site, ranging from −25 to −33 kcal mol^{-1}. In contrast, electrostatic contributions presented a more heterogeneous behavior. The differences in the electrostatic contributions between wild type and M244I, L248R, M351I, L384M and G398R mutants in simulations with imatinib can be attributed to changes in the amino acid solvation pattern, as indicated by the hydropathical character of the amino acids. Interestingly, some of the mutant amino acids resulted in a higher contribution to the electrostatic energy; these amino acids also presented the highest differences in the hydropathy values [52] (L248R=8.3; T315I=5.2; G398R=4.1; M244I=2.6; M351(I/T)=2.6 and L384M=1.9). With respect to the non-polar contributions, more negative values were found for nilotinib than for imatinib (except for M244I).

Role of the conserved water molecule

Schindler et al. [3] suggested that two different water molecules in the active site help to stabilize interactions between c-ABL and imatinib. However, only the one site (C_W), which established hydrogen bonds with the carbonyl oxygen atom of Asp381, the nitrogen atom of Lys271, and the side chain oxygen atom of Glu286 (interacting by a water bridge), was structurally conserved in the inactive protein in PDB 1OPJ. This fact prompted us to analyze the behavior of the water molecules at this specific site, focusing on their times of residence and substitutions by other water molecules during simulations with the wild type protein and five c-ABL mutants (L248R, T315I, T315S, M351T, and M351I) in complex with imatinib or nilotinib. The average residence time of each water molecule was very short, lasting typically 0.35 ~ 0.45 ps and exceptionally 3–4 ps. There were no differences between the residence times between the wild type and mutants, which were slightly higher in simulations with nilotinib when compared to imatinib. These data did not provide evidence for an association of mutations and resistance with the residence time of water molecules at the Cw crystallographic pocket.

Table 1 Experimental and predicted ΔG values for imatinib and nilotinib

Mutation	Experimental ΔG imatinib (*)	Predicted ΔG imatinib	Unsigned error	Predicted ΔG nilotinib
WT	−8.54	−7.57 (0.29)	0.97	−7.93 (0.27)
M244I	−8.03	−7.87 (0.47)	0.16	−8.03 (0.47)
M244V	−7.56	−6.89 (0.56)	0.67	−7.81 (0.30)
L248R	−6.45	−6.66 (0.48)	0.21	−7.35 (0.30)
Q252H	−7.60	−7.93 (0.26)	0.33	−8.03 (0.28)
Y253H	−6.52	−6.93 (0.26)	0.41	−7.31 (0.22)
E255K	−6.75	−6.88 (0.38)	0.13	−6.35 (0.38)
T315I	−6,45	−7.27 (0.40)	0.82	−7.90 (0.30)
T315S	−7.44	−7.75 (0.23)	0.31	−7.62 (0.30)
M351I	−7.95	−7.16 (0.70)	0.79	−7.70 (0.34)
M351T	−7.29	−6.76 (0.35)	0.53	−8.14 (0.45)
L384M	−7.62	−7.29 (0.35)	0.33	−7.87 (0.35)
G398R	−8.18	−7.82 (0.29)	0.36	−8.04 (0.38)

(*) Experimental IC_{50} values for c-ABL protein and mutants were retrieved from Azam et al. [49]. ΔG values were estimated according to $\Delta G \cong RT\ln(IC50)$ where T=300K, R =0.001987 kcal K^{-1} mol^{-1}. Figures in parenthesis account for total standard deviation of ΔG, calculated according to: $\sigma_{tot} = \sqrt{\beta^2(\sigma^2_{bound}(el) + \sigma^2_{free}(el)) + \alpha^2(\sigma^2_{bound}(vdw) + \sigma^2_{free}(vdw))}$, where α and β correspond to LIE coefficients and σ_x represents standard deviations for interaction terms in bound and free states. Comparison between experimental and calculated values for imatinib resulted in unsigned error less than 1.0 kcal mol^{-1}

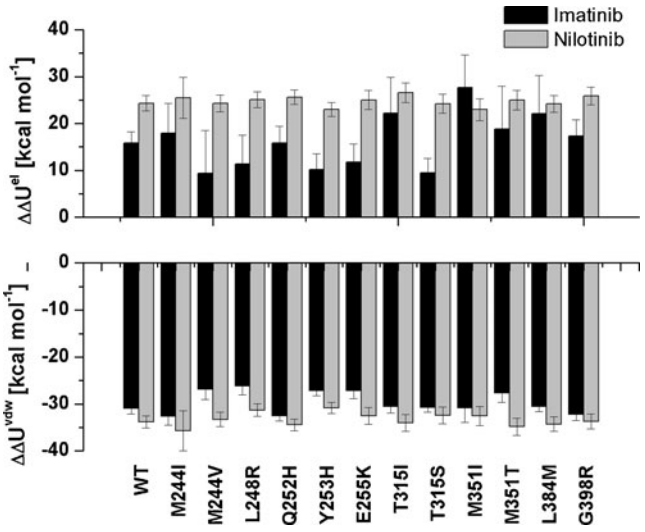

Fig. 2 Computed ligand-surrounding interactions of wild type (WT) and 12 mutations. The terms ΔU^{el} and ΔU^{vdwl} represent the variation of the electrostatic and non-polar contributions of the intermolecular energy, respectively, between free and bound states

On the other hand, when comparing wild type and mutants, the analysis of MD trajectories showed differences in the number of water molecules involved in the turn-over at the Cw pocket. Figure 3 shows the water molecules that turned-over at the Cw pocket during the simulations of 5 ns.

In the wild type protein, approximately 20 and 16 different water molecules occupied this site during simulations (5 ns) with imatinib and nilotinib, respectively. However, when simulations were performed with mutants, a higher number of different water molecules in turn-over were observed at this site. In simulations with imatinib, the number of water molecules involved in turn-over was 47 for L248R, 35 for T315I, 24 for T315S, 28 for M351T and 18 for M351I. In simulations with nilotinib, the number of water molecules was 17 for L248R, 26 for T315I, 10 for T315S, 29 for M351T and 23 for M351I. With respect to simulations with imatinib, these data showed a higher number of different water molecules in turn-over at the Cw pocket for mutants with higher IC50 estimates in in vitro experiments [50]. However, this trend was not found in simulations with nilotinib and the mutant T315I (with a IC50>2000 nM; data from O'Hare et al. [53]) or with the mutant M351T (with a IC50 of 7.8 nM; data from Redaelli et al. [54]). Nevertheless, an absence of experimental IC50 values for simulations with nilotinib for the remaining mutants did not allow for a better evaluation.

When considering only imatinib simulations, the relationship between the numbers of different water molecules in turn-over at the Cw initial position may be associated with structural changes. This scenario was particularly evident for mutations at two positions, 315 and 351, where two different amino acid substitutions for each position resulted in different levels of resistance. At position 315, the T315I mutation certainly produced a more drastic change than T315S, reflected in a large IC50 value (> 20 μM and 3.8 μM, respectively) and in a large number of different water molecules involved in the turn-over at Cw pocket. The same rationale can be applied to M351S and M351T mutations.

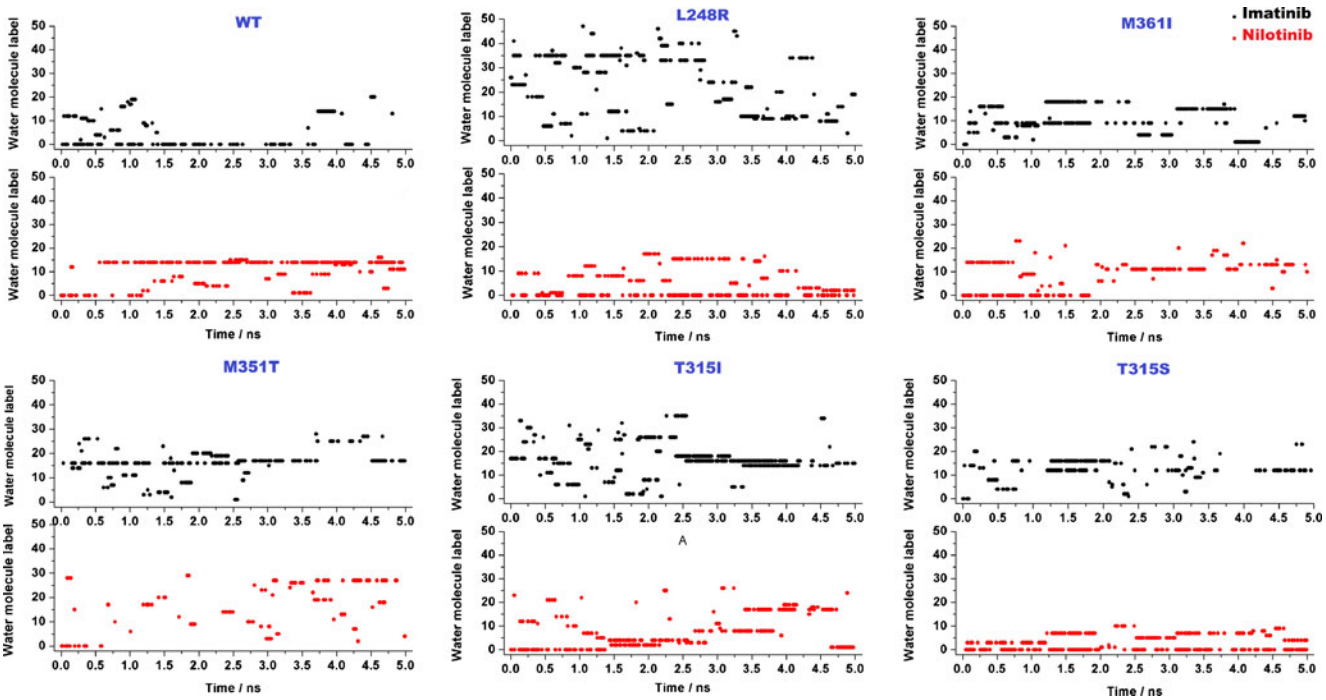

Fig. 3 Time evolution of the water molecules in turn-over of the crystallographic water Cw (label 0) in the vicinity of imatinib (black) and nilotinib (red), for the WT , L248R, M351I, M351T, T315I, and T315S mutations

Conclusions

In this work, we have studied the effects of c-ABL mutants in complex with two ligands, imatinib and nilotinib, by thermodynamic and structural analyses.

The linear interaction energy method proved to be adequate for differentiating the effectiveness of both ligands by means of $\Delta\Delta G$ calculations and confirmed the higher potency of nilotinib over imatinib, except for mutations T315S and E255K. Despite the fact that experimental findings could have been partially reproduced, modeling mutations that are spread across the binding site by means of a single multivariate model is a challenging task. Although we were not able to obtain a strict reproduction of the $\Delta\Delta G_{(mut\text{-}wt)}$ values, the model was consistent with the majority of the experimental results. However, this model presents limitations because of the small size of the population (a low number of mutations), the spatial distribution of mutations in different places in the structure, and the inability to evaluate the effect of mutations in the structure beyond the simulation sphere.

The presence of water molecules at the Cw pocket, delimited by residues Glu286, Lys271 and Asp381, was not found to be directly associated with the stability of the binding of ligands with c-ABL. No association was found between the residence time of a water molecule at the Cw pocket and drug resistance, because equivalent residence times were found for mutant c-ABL proteins. Finally, the physicochemical characteristics of mutated residues, along with their size, can contribute to the resistance experienced by these ligands. Substitutions by larger amino acids than those found in the wild type enhanced the number of water molecules turning-over at the Cw pocket and were associated with a lower effective inhibition of kinase activity.

Acknowledgments Swiss-Bridge Foundation, Conselho Nacional de Desenvolvimento Científico e Tecnológico CNPq (304403/2008-3, 473914/2008-5), Convênio Instituto Nacional de Câncer – Fundação Oswaldo Cruz (INCA-FIOCRUZ), Ministry of Health, Pesquisa para o Sistema Único de Saúde - Fundação Carlos Chagas Filho de Amparo à Pesquisa do Estado do Rio de Janeiro (PP-SUS-FAPERJ and Programa de Computação Científica (PROCC) da Fundação Oswaldo Cruz (FIOCRUZ) supported this work. The authors want to thank Dr. Héctor Seuanez Abreu for manuscript review.

References

1. Pear WS, Miller JP, Xu LW, Pui JC, Soffer B, Quackenbush RC, Pendergast AM, Bronson R, Aster JC, Scott ML, Baltimore D (1998) Efficient and rapid induction of a chronic myelogenous leukemia-like myeloproliferative disease in mice receiving P210 bcr/abl-transduced bone marrow. Blood 92:3780–3792
2. Druker BJ, Tamura S, Buchdunger E, Ohno S, Segal GM, Fanning S, Zimmermann J, Lydon NB (1996) Effects of a selective inhibitor of the Abl tyrosine kinase on the growth of Bcr-Abl positive cells. Nat Med 2:561–566
3. Schindler T, Bornmann W, Pellicena P, Miller WT, Clarkson B, Kuriyan J (2000) Structural mechanism for STI-571 inhibition of Abelson tyrosine kinase. Science 289:1938–1942
4. Druker BJ, Talpaz M, Resta DJ, Peng B, Buchdunger E, Ford JM, Lydon NB, Kantarjian H, Capdeville R, Ohno-Jones S, Sawyers CL (2001) Efficacy and safety of a specific inhibitor of the BCR-ABL tyrosine kinase in chronic myeloid leukemia. N Engl J Med 344:1031–1037
5. Gorre ME, Mohammed M, Ellwood K, Hsu N, Paquette R, Rao PN, Sawyers CL (2001) Clinical resistance to STI-571 cancer therapy caused by BCR-ABL gene mutation or amplification. Science 293:876–880
6. Branford S, Rudzki Z, Walsh S, Grigg A, Arthur C, Taylor K, Herrmann R, Lynch KP, Hughes TP (2002) High frequency of point mutations clustered within the adenosine triphosphate-binding region of BCR/ABL in patients with chronic myeloid leukemia or Ph-positive acute lymphoblastic leukemia who develop imatinib (STI571) resistance. Blood 99:3472–3475
7. Branford S, Rudzki Z, Walsh S, Parkinson I, Grigg A, Szer J, Taylor K, Herrmann R, Seymour JF, Arthur C, Joske D, Lynch K, Hughes T (2003) Detection of BCR-ABL mutations in patients with CML treated with imatinib is virtually always accompanied by clinical resistance, and mutations in the ATP phosphate-binding loop (P-loop) are associated with a poor prognosis. Blood 102:276–283
8. Nicolini FE, Corm S, Le QH, Sorel N, Hayette S, Bories D, Leguay T, Roy L, Giraudier S, Tulliez M, Facon T, Mahon FX, Cayuela JM, Rousselot P, Michallet M, Preudhomme C, Guilhot F, Roche-Lestienne C (2006) Mutation status and clinical outcome of 89 imatinib mesylate-resistant chronic myelogenous leukemia patients: a retrospective analysis from the French intergroup of CML (Fi(phi)-LMC GROUP). Leukemia 20:1061–1066
9. Manley PW, Cowan-Jacob SW, Buchdunger E, Fabbro D, Fendrich G, Furet P, Meyer T, Zimmermann J (2002) Imatinib: a selective tyrosine kinase inhibitor. Eur J Cancer 38:S19–S27
10. Nagar B, Bornmann WG, Pellicena P, Schindler T, Veach DR, Miller WT, Clarkson B, Kuriyan J (2002) Crystal structures of the kinase domain of c-Abl in complex with the small molecule inhibitors PD173955 and imatinib (STI-571). Cancer Res 62:4236–4243
11. Cowan-Jacob SW, Fendrich G, Floersheimer A, Furet P, Liebetanz J, Rummel G, Rheinberger P, Centeleghe M, Fabbro D, Manley PW (2007) Structural biology contributions to the discovery of drugs to treat chronic myelogenous leukaemia. Acta Crystallogr D 63:80–93
12. Weisberg E, Manley PW, Cowan-Jacob SW, Hochhaus A, Griffin JD (2007) Second generation inhibitors of BCR-ABL for the treatment of imatinib-resistant chronic myeloid leukaemia. Nat Rev Cancer 7:345–356
13. Kantarjian HM, Gattermann N, Hochhaus A, Larson R, Rafferty T, Weitzman A, Haque A, Giles F, O'Brien SG, le Coutre P (2006) A phase II study of nilotinib a novel tyrosine kinase inhibitor administered to imatinib-resistant or intolerant patients with chronic myelogenous leukemia (CML) in accelerated phase (AP). Blood 108:615a–616a
14. le Coutre P, Bhalla K, Giles F, Baccarani M, Ossenkoppele GJ, Hochhaus A, Gattermann N, Rafferty T, Haque A, Weitzman A, Kantarjian H (2006) A phase II study of nilotinib, a novel tyrosine kinase inhibitor administered to imatinib-resistant and -intolerant patients with chronic myelogenous leukemia (CML) in chronic phase (CP). Blood 108:53a–53a
15. Cortes J, Kantarjian HM, Baccarani M, Brummendorf TH, Liu DL, Ossenkoppele G, Volkert ADG, Hewes B, Moore L, Zacharchuk C, Gambacorti C (2006) A phase 1/2 study of SKI-606, a dual inhibitor of src and abl kinases, in adult patients with Philadelphia chromosome positive (Ph+) chronic myelogenous leukemia

(CML) or acute lymphocytic leukemia (ALL) relapsed, refractory or intolerant of imatinib. Blood 108:54a–54a
16. Cortes J, Kim DW, Guilhot F, Rosti G, Silver RT, Gollerkeri A, Agarwal P, Branford S, Apperley JF (2006) Dasatinib (SPRYCEL (R)) in patients (pts) with chronic myelogenous leukemia in accelerated phase (AP-CML) that is imatinib-resistant (im-r) or -intolerant (im-i): updated results of the CA180-005 'START-A' phase II study. Blood 108:613a–613a
17. Cortes JE, Kim DW, Rosti G, Rousselot P, Bleickardt E, Zink R, Sawyers C (2006) Dasatinib (D) in patients (pts) with chronic myelogenous leukemia (CML) in myeloid blast crisis (MBC) who are imatinib-resistant (IM-R) or IM-intolerant (IM-I): results of the CA180006 'START-B' study. J Clin Oncol 24:344s–344s
18. Golas JM, Arndt K, Etienne C, Lucas J, Nardin D, Gibbons J, Frost P, Ye F, Boschelli DH, Boschelli F (2003) SKI-606, a 4-anilino-3-quinolinecarbonitrile dual inhibitor of Src and Abl kinases, is a potent antiproliferative agent against chronic myelogenous leukemia cells in culture and causes regression of K562 xenografts in nude mice. Cancer Res 63:375–381
19. Talpaz M, Shah NP, Kantarjian H, Donato N, Nicoll J, Paquette R, Cortes J, O'Brien S, Nicaise C, Bleickardt E, Blackwood-Chirchir MA, Iyer V, Chen TT, Huang F, Decillis AP, Sawyers CL (2006) Dasatinib in imatinib-resistant Philadelphia chromosome-positive leukemias. N Engl J Med 354:2531–2541
20. Giles F, Cortes J, Bergstrom DA, Xiao A, Bristow P, Jones D, Verstovsek S, Thomas D, Kantarjian H, Freedman SJ (2006) MK-0457, a novel aurora kinase and BCR-ABL inhibitor, is active against BCR-ABL T315I mutant chronic myelogenous leukemia (CML). Blood 108:52a–52a
21. Ray A, Cowan-Jacob SW, Manley PW, Mestan J, Griffin JD (2007) Identification of BCR-ABL point mutations conferring resistance to the Abl kinase inhibitor AMN107 (nilotinib) by a random mutagenesis study. Blood 109:5011–5015
22. Weisberg E, Manley P, Mestan J, Cowan-Jacob S, Ray A, Griffin JD (2006) AMN107 (nilotinib): a novel and selective inhibitor of BCR-ABL Brit J. Cancer 94:1765–1769
23. Pricl S, Fermeglia M, Ferrone M, Tamborini E (2005) T315I-mutated Bcr-Abl in chronic myeloid leukemia and imatinib: insights from a computational study. Mol Cancer Ther 4:1167–1174
24. Aleksandrov A, Simonson T (2010) A molecular mechanics model for imatinib and imatinib:kinase binding. J Comput Chem 31:1550–1560
25. Aleksandrov A, Simonson T (2010) Molecular dynamics simulations show that conformational selection governs the binding preferences of imatinib for several tyrosine kinases. J Biol Chem 285:13807–13815
26. Åqvist J, Medina C, Samuelsson JE (1994) A new method for predicting binding affinity in computer-aided drug design. Protein Eng 7:385–391
27. Knight JDR, Hamelberg D, McCammon JA, Kothary R (2009) The role of conserved water molecules in the catalytic domain of protein kinases. Proteins 76:527–535
28. Shaltiel S, Cox S, Taylor SS (1998) Conserved water molecules contribute to the extensive network of interactions at the active site of protein kinase A. Proc Natl Acad Sci USA 95:484–491
29. Loris R, Langhorst U, De Vos S, Decanniere K, Bouckaert J, Maes D, Transue TR, Steyaert J (1999) Conserved water molecules in a large family of microbial ribonucleases. Proteins 36(1):117–134
30. Beria I, Ballinari D, Bertrand JA, Borghi D, Bossi RT, Brasca MG, Cappella P, Caruso M, Ceccarelli W, Ciavolella A, Cristiani C, Croci V, De Ponti A, Fachin G, Ferguson RD, Lansen J, Moll JK, Pesenti E, Posteri H, Perego R, Rocchetti M, Storici P, Volpi D, Valsasina B (2010) Identification of 4,5-Dihydro-1H-pyrazolo[4,3-h]quinazoline derivatives as a new class of orally and selective polo-like kinase 1 inhibitors. J Med Chem 53:3532–3551
31. Szep S, Park S, Boder ET, Van Duyne GD, Saven JG (2009) Structural coupling between FKBP12 and buried water. Proteins 74:603–611
32. Rodriguez-Almazan C, Arreola R, Rodríguez-Larrea D, Aguirre-López B, Gómez-Puyou MT, Perez-Montfort R, Costas M, Gomez-Puyou A, Torres-Larios A (2008) Structural basis of human triosephosphate isomerase deficiency: mutation E104D is related to alterations of a conserved water network at the dimer interface. J Biol Chem 283:23254–23263
33. Shan YB, Seeliger MA, Eastwood MP, Frank F, Xu HF, Jensen MO, Dror RO, Kuriyan J, Shaw DE (2009) A conserved protonation-dependent switch controls drug binding in the Abl kinase. Proc Natl Acad Sci USA 106:139–144
34. Brandsdal BO, Österberg F, Almlöf M, Feierberg I, Luzhkov VB, Åqvist J (2003) Free energy calculations and ligand binding. Adv Protein Chem 66:123–158
35. Singh N, Warshel A (2010) Absolute binding free energy calculations: on the accuracy of computational scoring of protein-ligand interactions. Proteins 78:1705–1723
36. Nagar B, Hantschel O, Young MA, Scheffzek K, Veach D, Bornmann V, Clarkson B, Superti-Furga G, Kuriyan J (2003) Structural basis for the autoinhibition of c-Abl tyrosine kinase. Cell 112:859–871
37. Guex N, Peitsch MC (1997) SWISS-MODEL and the Swiss-PdbViewer: an environment for comparative protein modeling. Electrophoresis 18:2714–2723
38. Weisberg E, Manley PW, Breitenstein W, Bruggen J, Cowan-Jacob SW, Ray A, Huntly B, Fabbro D, Fendrich G, Hall-Meyers E, Kung AL, Mestan J, Daley GQ, Callahan L, Catley L, Cavazza C, Mohammed A, Neuberg D, Wright RD, Gilliland DG, Griffin JD (2005) Characterization of AMN107, a selective inhibitor of native and mutant Bcr-Abl. Cancer Cell 7:129–141
39. Marelius J, Kolmodin K, Feierberg I, Åqvist J (1998) Q: a molecular dynamics program for free energy calculations and empirical valence bond simulations in biomolecular systems. J Mol Graph Model 16:213–225
40. Daura X, Mark AE, van Gunsteren WF (1998) Parameterization of aliphatic CHn united atoms of GROMOS96 force field. J Comput Chem 19:535–547
41. Schüttelkopf AW, van Aalten DMF (2004) PRODRG - a tool for high-throughput crystallography of protein-ligand complexes. Acta Crystallogr D60:1355–1363
42. Halgren TA (1996) Merck molecular force field 2. MMFF94 van der Waals and electrostatic parameters for intermolecular interactions. J Comput Chem 17:520–552
43. Berendsen HJC, Postma JPM, van Gunsteren WF, Hermans J (1981) In: Pullman B, Pullman A (eds) Intermolecular forces. Springer, Heidelberg, p 584
44. Lee FS, Warshel A (1992) A local reaction field method for fast evaluation of long-range electrostatic interactions in molecular simulations. J Chem Phys 97:3100–3107
45. Berendsen H, Postma J, Van Gunsteren W, Dinola A, Haak J (1984) Molecular dynamics with coupling to an external bath. J Chem Phys 81:3684–3690
46. Ryckaert JP, Ciccotti G, Berendsen HJC (1977) Numerical-integration of cartesian equations of motion of a system with constraints - molecular-dynamics of N-alkanes. J Comput Phys 23:327–341
47. Allen MP, Tildesley DJ (1987) Computer simulation of liquids. Clarendon Press, Oxford University Press, New York, p 385
48. Hansson T, Marelius J, Åqvist J (1998) Ligand binding affinity prediction by linear interaction energy methods. J Comput Aided Mol Des 12:27–35
49. Azam M, Latek RR, Daley GQ (2003) Mechanisms of autoinhibition and STI-571/imatinib resistance revealed by mutagenesis of BCR-ABL. Cell 112:831–843
50. Lee TS, Potts SJ, Kantarjian H, Cortes J, Giles F, Albitar M (2008) Molecular basis explanation for imatinib resistance of BCR-ABL

due to T3151 and P-loop mutations from molecular dynamics simulations. Cancer 112:1744–1753
51. Almlof M, Aqvist J, Smalas AO, Brandsdal BO (2006) Probing the effect of point mutations at protein-protein interfaces with free energy calculations. Biophys J 90:433–442
52. Kyte J, Doolittle RF (1982) A simple method for displaying the hydropathic character of a protein. J Mol Biol 157:105–132
53. O'Hare T, Eide CA, Deininger MWN (2007) Bcr-Abl kinase domain mutations, drug resistance, and the road to a cure for chronic myeloid leukemia. Blood 110:2242–2249
54. Redaelli S, Piazza R, Rostagno R, Magistroni V, Perini P, Marega M, Gambacorti-Passerini C, Boschelli F (2009) Activity of bosutinib, dasatinib, and nilotinib against 18 imatinib-resistant BCR/ABL mutants. J Clin Oncol 27:469–471